Energy Proceedings
Vol 38, 2024
ISSN 2004-2965

Numerical Simulation of Poiseuille-Rayleigh-Benard Convection for Density Extreme Fluid in a Horizontal Rectangular Channel

Yu-Zhi Zhu[1], Si-Bo Wan[2], You-Rong Li[1*]

1 School of Energy and Power Engineering, Chongqing University, Chongqing 400044, China

*Corresponding Author: liyourong@cqu.edu.cn

ABSTRACT

A series of three-dimensional numerical simulations of Poiseuille-Rayleigh-Benard (P-R-B) convection of cold water with different aspect ratios were carried out by using the finite volume method. The results indicate that the flow weakens gradually as the density inversion parameter increases, indicating that the density inversion parameter has a suppression effect on secondary flow. The average Nusselt number in the fully developed region increases with the increasing Rayleigh number and aspect ratio and the decreasing density inversion parameter. Based on the calculation results, a heat transfer correlation for the fully developed region of P-R-B convection was obtained.

Keywords: P-R-B convection, density inversion parameter, aspect ratio, heat transfer

1. INTRODUCTION

When the temperature difference exceeds a critical value, Rayleigh-Benard (R-B) convection will occur in the horizontal fluid layer where the lower surface is heated and the upper plane is cooled. If there is also a directional Poiseuille flow throughout the liquid layer, it is called Poiseuille-Rayleigh-Benard (P-R-B) convection. P-R-B convection has attracted much attention due to its widespread application in industrial production such as solar collectors, cooling of electronic components, and chemical vapor deposition of thin films or coatings prepared on heating substrates.

Mergui et al. [1] analyzed the generation mechanism of longitudinal roll, and found that the longitudinal rolls always start to develop from the velocity boundary layer near the two side walls of the entrance. Benderradji et al. [2] found that the longitudinal rolls are caused by the side wall effect and the supercritical vertical gradient in the bottom boundary layer. Taher et al. [3] gave a relationship between the characteristic length and Rayleigh (*Ra*) and Reynolds (*Re*) numbers at the beginning of the instability zone of P-R-B convection of water.

In P-R-B convection, various flow patterns will change the heat and mass transfer characteristics, resulting in uneven distribution of wall temperature or heat flux, thereby affecting industrial production processes. Therefore, scholars have conducted in-depth studies on heat transfer characteristics. Boulemtafes Boukadoum et al. [4] found that the heat transfer in the solar air heater can be enhanced or weakened, depending on the aspect ratio. Taher et al. [5] established a heat transfer correlation of Nusselt number in the fully developed zone of longitudinal roll of normal temperature water through experiments. Nicolas and Mergui [6] regulated the flow pattern structure by introducing harmonic mechanical excitation at the inlet to obtain more uniform time averaged heat transfer, the effect of which was mainly related to *Re*, *Ra*, disturbance frequency and amplitude, etc.

In all the above studies, the working fluids used are conventional fluids that meet Boussinesq approximation, while there are few studies on P-R-B convection with density extreme fluids. Cold water is a commonly used cold storage and cooling medium, which flows as a working fluid in the channel and continuously conducts convective heat transfer with circuit boards and heat absorbers. Conducting research on its flow characteristics and heat transfer performance, and analyzing the influence of density inversion parameters, is crucial for improving the cooling effect of electronic components and the thermal efficiency of solar water heaters.

2. PHYSICAL MATHEMATICAL MODEL

The physical model is shown in Fig. 1. The horizontal channel with length *l*, width *b* and height *h* is composed of the heating section and the adiabatic inlet section which allows the development of Poiseuille flow. The top surface of the heating section maintains a lower

This is a paper for 15th International Conference on Applied Energy (ICAE2023), Dec. 3-7, 2023, Doha, Qatar.

temperature T_c, the bottom is a higher temperature T_h, and the other walls are insulated. The fluid with a temperature of T_m flows into the adiabatic inlet section, where T_m is the temperature corresponding to the maximum density.

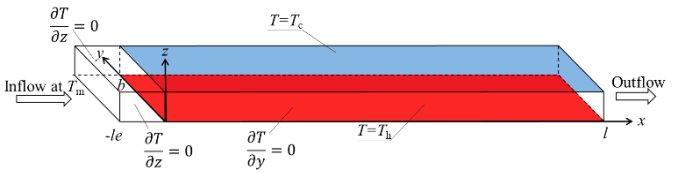

Fig. 1. Physical model

To simplify the model, the following assumptions are introduced. (1) The cold water is incompressible Newtonian fluid, and the flow is laminar. (2) Except for the density in the buoyancy term, all physical parameters are constants. (3) No-slip velocity condition is set on all solid walls and the viscous dissipation is neglected.

The density of cold water in the buoyancy term adopts the nonlinear density formula proposed in Ref.[7], which varies with temperature as follows

$$\rho(T) = \rho_m\left(1 - \gamma\left|T - T_m\right|^q\right), \tag{1}$$

where γ=9.297173×10^{-6}(℃)$^{-q}$, ρ_m=999.972kg/m^3, T_m=4.029325℃, and q=1.894816. In addition, the other thermophysical properties are taken as the values at the reference temperature T_m, as shown in Table 1.

Table 1. Thermophysical properties of cold water at T_m

Physical parameters	symbol	value	unit
Thermal conductivity	λ	0.569	W/(m·K)
kinematic viscosity	v	1.567×10^{-6}	m^2/s
Thermal diffusivity	α	1.354×10^{-7}	m^2/s
Prandtl number	Pr	11.573	-

Taking h, u_m, ρu_m^2 and h/u_m as the dimensionless reference scales for length, velocity, pressure and time, dimensionless governing equations can be expressed as

$$\nabla\cdot\boldsymbol{V} = 0, \tag{2}$$

$$\frac{\partial\boldsymbol{V}}{\partial\tau} + (\boldsymbol{V}\cdot\nabla)\boldsymbol{V} = -\nabla P + \frac{1}{Re}\nabla^2\boldsymbol{V} + \frac{Ra}{Pr\,Re^2}\left|\Theta - \Theta_m\right|^q \boldsymbol{e}_z, \tag{3}$$

$$\frac{\partial\Theta}{\partial\tau} + \boldsymbol{V}\cdot\nabla\Theta = \frac{1}{PrRe}\nabla^2\Theta, \tag{4}$$

here Pr, Θ_m, Ra and Re are respectively Prandtl number, density inversion parameter, Rayleigh number and Reynolds number,

$$Pr = \frac{v}{\alpha},\quad \Theta_m = \frac{T_m - T_c}{T_h - T_c},\quad Ra = \frac{g\gamma(\Delta T)^q h^3}{\alpha v},\quad Re = \frac{u_m h}{v}. \tag{5}$$

The initial condition is given by

$$\tau = 0,\ U = 1,\ V = W = 0,\ \Theta = \Theta_m. \tag{6}$$

The heat transfer performance can be described by the average Nusselt number ($Nu_{m,sp}$) in the span direction, which is defined as follows

$$Nu_{m,sp} = \frac{1}{B}\int_0^B Nu\,dY, \tag{7}$$

where B is aspect ratio of the channel, B=b/h.

The governing equations are solved by finite volume method. The SIMPlE algorithm is used to handle the coupling between velocity and pressure. The QUICK scheme and the central difference scheme are used for the convection terms and the diffusion terms, respectively. A fixed time step is used for numerical calculation. When the relative error between the two iterations of temperature and velocity is less than 10^{-5}, the calculation is considered to be convergent.

To examine the numerical method, numerical calculations were conducted on P-R-B convection with Pr=6.4, Re=1.02 and Ra=3494. The vertical velocity distribution along the span direction at X=15.7 and Z=0.5 obtained from the calculations was in good agreement with the experimental results of Ouazzani et al. [8].

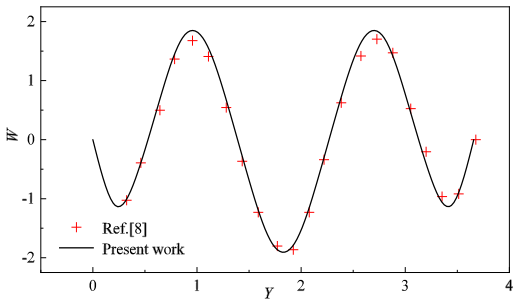

Fig. 2. Distribution of vertical velocity along the span direction at X=15.7 and Z=0.5

3. RESULTS AND DISCUSSION

Figure 3 shows the distribution of dimensionless vertical velocity W along the span direction. With the increase of the density inversion parameter Θ_m, W gradually decreases, indicating that Θ_m has an inhibitory effect on secondary flow. Furthermore, the larger Θ_m is, the more obvious the inhibitory effect is. The flow inhibition effect at Θ_m=0.1 is smaller than those at Θ_m=0.3 and 0.5. The central roll in the flow channel splits and produces a pair of additional rolls, which minimizes the total energy of the system and maintains its stability. As Ra increases, the vertical temperature difference increases, and the buoyancy effect increases. Therefore, the amplitude of W increases.

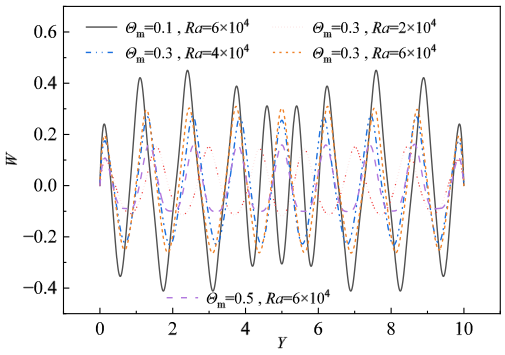

Fig. 3. Dimensionless vertical velocity W along the span direction at different Θ_m and Ra when Re=20 and B=10

Figure 4 shows the variation of the maximum stream function with density inversion parameter. In channels with different aspect ratios, when the density inversion parameter is small, the suppression effect of the density inversion characteristic on the secondary flow becomes weak. With the increase of the density inversion parameter, the suppression effect of the stable fluid layer above the density extreme plane on the entire system will be more intense, and the secondary flow intensity in the channel will decrease. The maximum stream function will sharply decrease. In addition, it increases gradually with the increase of Ra, indicating that the flow strength on the cross-section is closely related to the buoyancy. The larger the buoyancy is, the stronger the secondary flow is.

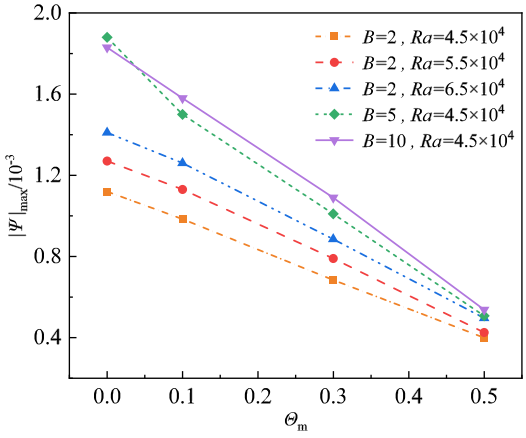

Fig. 4. The variation of the maximum stream function at X=110 with Θ_m when Re=25

Figure 5 shows the variation of the average Nu in the span direction along X direction. Obviously, the variation of the average Nu at different aspect ratios is similar. Near the entrance, the thermal boundary layer near bottom is continuously thickened along the flow direction, and Nu decreases gradually. With the appearance of buoyancy convection, Nu gradually increases, and finally reaches a constant value. As the density inversion parameter increases, the temperature difference between the fluid and the lower surface decreases, the temperature non-uniformity in the flow channel becomes smaller. The buoyancy effect is weakened, and the average Nu decreases. The average Nu increases significantly with the increasing Ra. This is because the larger Ra is, the stronger the buoyancy effect in the flow is. The fluid scours the thermal boundary layer near the upper and lower surfaces with a greater vertical velocity, which enhances the heat transfer in the flow channel. The greater Re is, the higher the flow velocity of the fluid in the channel is. Therefore, the boundary layer becomes the thinner, and the establishment length of the longitudinal roll and the fully developed length of the mixed convection increase. When the boundary layer is fully developed, Nu does not change with Re.

The overall heat transfer performance of P-R-B convection can be measured by the average Nu in the fully developed region. Fig. 6 shows the variation of the average Nu in the fully developed region with Ra. The average Nu at different density inversion parameters and aspect ratios increases with the increasing Ra.

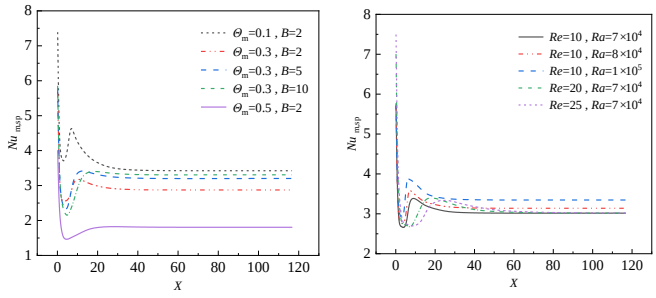

(a)Re=10, Ra=6×10^4 (b)B=2, Θ_m=0.3

Fig.5. The variations of the average Nu along X direction

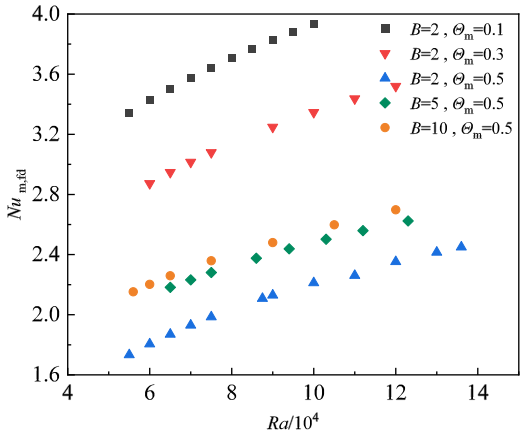

Fig. 6. The variation of average Nu in fully developed region with Ra

Figure 7 shows the variation of the average *Nu* in the fully developed region with the aspect ratio *B*. As *B* increases, *Nu* in fully developed region increases, but the increasing magnitude gradually decreases. This is because when the aspect ratio is small, under the strong restriction of the sidewall, the flow weakens and the heat transfer ability is poor. As the aspect ratio increases, more convective rolls are formed in the flow channel, and the flow and mixing of the fluid are stronger. Moreover, the restriction of the sidewall gradually weakens, the flow becomes stronger and the heat transfer ability is significantly enhanced. Therefore, in engineering applications, it is possible to operate under conditions with small density inversion parameters and moderate channel geometry to effectively enhance heat transfer in the channel.

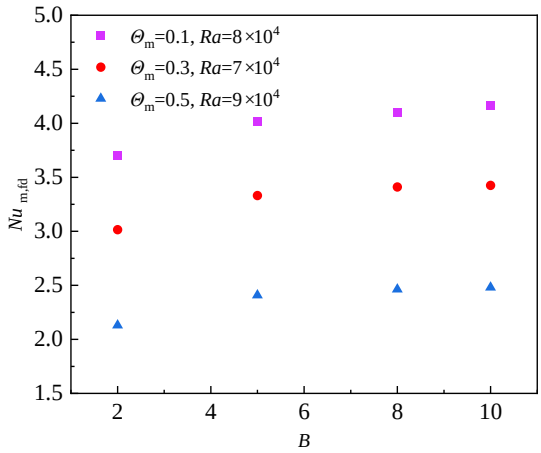

Fig. 7. Variations of the average *Nu* in the fully developed region with *B* at different Θ_m

According to the calculated results, a heat transfer correlation of the average Nusselt number $Nu_{m,fd}$ in the fully developed region with respect to the density inversion parameter Θ_m, *Ra* and *B* is fitted, in the following form

$$Nu_{m,fd} = (3 + 0.405B)(0.0468 - 0.0642\Theta_m)Ra^{(0.282-0.005B+0.098\Theta_m)} \quad (8)$$

The formula is suitable for the P-R-B convection of cold water in the horizontal rectangular channel within the ranges of $2 \le B \le 10$, $10 \le Re \le 25$, $0.1 \le \Theta_m \le 0.5$ and $5.5\times10^4 \le Ra \le 1.36\times10^5$. Fig. 8 shows the comparison between the numerical results of *Nu* in the fully developed region and the fitting results, and the error is within ±7%.

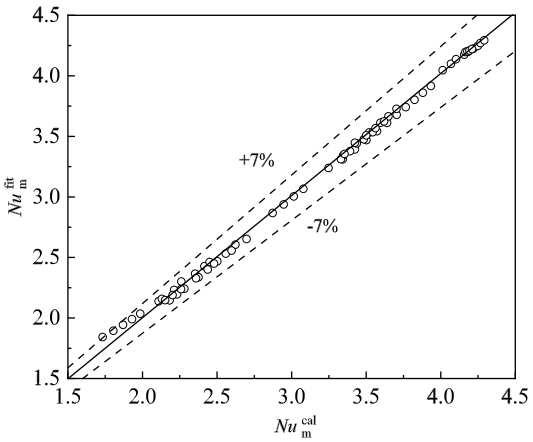

Fig. 8. Comparison of numerical results and fitting results of the average *Nu*

4. CONCLUSIONS

Based on numerical simulation of P-R-B convection of density extreme fluid in horizontal rectangular channels with different *B*, the results show that

(1) Under different B, as the density inversion parameter increases, the dimensionless vertical velocity and the maximum stream function gradually decrease, indicating that the density inversion parameter has a suppression effect on secondary flow. The larger the density inversion parameter is, the more obvious the suppression effect is.

(2) As the density inversion parameter increases, the average *Nu* in the span direction decreases, and the heat transfer significantly decreases. *Nu* in the fully developed region does not change with *Re*.

(3) The average *Nu* in the fully developed region increases with the increasing *Ra* and *B*, but decreases with the increasing Θ_m. Based on the numerical results, a correlation of the average *Nu* with Θ_m, *Ra* and *B* in the fully developed region was obtained.

ACKNOWLEDGEMENT

This work is supported by the National Natural Science Foundation of China (Grant No. 52076017)

DECLARATION OF INTEREST STATEMENT

The authors declare that they have no known competing financial interests or personal relationships that could have appeared to influence the work reported in this paper. All authors read and approved the final manuscript.

REFERENCE

[1] Mergui S, Nicolas X, Hirata S. Sidewall and thermal boundary condition effects on the evolution of longitudinal rolls in Rayleigh-Benard-Poiseuille convection. Phys Fluids 2011; 23 (8): 084101.

[2] Benderradji A, Haddad A, Taher R, Medale M, Abid C, Papini F. Characterization of fluid flow patterns and heat transfer in horizontal channel mixed convection. Heat Mass Transfer 2008; 44: 1465-76.

[3] Taher R, Ahmed MM, Haddad Z, Abid C. Poiseuille-Rayleigh-Benard mixed convection flow in a channel: Heat transfer and fluid flow patterns. I J Heat Mass Transf 2021; 180: 121745.

[4] Boulemtafes-Boukadoum A, Abid C, Benzaoui A. 3D numerical study of the effect of aspect ratio on mixed convection air flow in upward solar air heater. Int J Heat Fluid Fl 2020; 84: 108570.

[5] Taher R, Abid C. Experimental determination of heat transfer in a Poiseuille-Rayleigh-Bénard flows. Heat Mass Transfer 2018; 54: 1453-1466.

[6] Nicolas X, Mergui S. Harmonic mechanical excitations of steady convective instabilities: A means to get more uniform heat transfers in mixed convection flows?. I J Heat Mass Transf 2014; 77: 419-38.

[7] Gebhart B, Mollendorf JC. New density relation for pure and saline water. Deep Sea Res 1977; 24(9): 831-848.

[8] Ouazzani MT, platten JK, mojtabi A. Experimental-study of mixed convection between 2 horizontal plates at different temperatures-II. I J Heat Mass Transf 1990; 33(7): 1417-1427.